

Crystallographic data on axially compressed Kevlar 49 fibres

R V IYER, KALYANI VIJAYAN*, K SOORYANARAYANA⁵ and T N GURU ROW*

Materials Science Division, National Aerospace Laboratories, Bangalore 560017, India

=Solid State and Structural Chemistry Unit, Indian Institute of Science, Bangalore 560012, India

MS received 17 December 1998

Abstract. Axially compressed Kevlar 49 fibres have been examined by X-ray diffraction methods. The most prominent effect of axial compression is the anisotropic deformation of the unit cell. Whereas the c-axial length, which corresponds to the chain axis, undergoes contraction, the basal plane dimensions manifest enlargement. The deformations increase with the extent of axial compression. The half-widths and the azimuthal spread of reflections also exhibit changes. The compression induced structural changes provide qualitative support to the experimentally observed reduction in tensile strength and modulus.

Keywords. Kevlar; ultrasonic; compression; unit cell; tensile properties; deformation.

1. Introduction

It is well known that in contrast to their exceptional tensile characteristics, the compressive properties of Kevlar fibres are poor. Detailed investigations have been carried out in the past to understand the deformation characteristics of axially compressed Kevlar 49 fibres. Greenwood and Rose (1974) who were the first to study the compressive behaviour of Kevlar 49 fibres showed that kink bands characterized the surface of fibres compressed by the elastica loop method. They also reported the separation of fibrils under the compressed surface. Dobb *et al* (1981) examined the fibres compressed by the loop method as well as those extracted from axially compressed fibre-epoxy resin composites. The deformation mechanism proposed by them is also based on the initial formation of kink bands. From an extensive study of the longitudinal sections of compressed fibres, they showed that the propagation of compression induced kink bands is unaffected by the presence of pleated structure which characterizes Kevlar 49 fibres (Dobb *et al* 1977). They also reported the presence of micro cracks in the kink bands and delamination in fibres initially compressed and subsequently fractured in tension. Deteresa *et al's* (1984) study which used the bending beam method to compress the fibres, also confirmed the occurrence of kink bands on the surface. They view the kink formation as due to buckling of the microfibrils. The later work of McGarry and Moalli (1991) provides further evidence for the formation of kink bands by buckling of fibrils at or very near the surface of the

fibre. They examined the effect of coating of the surface on the compressive strength of the fibre. The recent work of Iyer and Vijayan (1996) also confirmed the occurrence of kink bands, fibrillation and macrobuckling in ultrasonically compressed Kevlar fibres. All these investigations have established that buckling of fibrils and the resultant formation of kink bands are the prominent manifestations of axial compression of Kevlar fibres.

It must be pointed out that the macro characteristics of compressed Kevlar 49 fibres reported so far in literature are based primarily on optical and electron microscopic observations. To date, crystallographic data on compressed fibres are not available. As is well known, in the architecture of fibre morphology, fibrils include several crystallites and each crystallite includes several crystallographic unit cells. When fibres undergo axial compression does the effect percolate down to the crystal lattice? This question was addressed and the results emerging from the first X-ray diffraction study on axially compressed Kevlar 49 fibres are presented in this paper.

2. Experimental

The samples used in this study were Kevlar 49 fibres made commercially available by DuPont Inc., USA. Details of ultrasonic compression of Kevlar fibres have been reported elsewhere (Iyer and Vijayan 1996). Axially compressed fibres were characterized primarily by X-ray diffraction methods and supported by few tensile testing.

X-ray diffraction patterns were recorded both prior to and after various extents of compression, using a STOEISTADI-P powder diffractometer with transmission geometry (fine focus setting). Germanium monochromated CuK α_1 radiation was employed. X-ray diffraction data

Paper presented at the 5th IUMRS-ICA 98 International conference held at Bangalore, October 1998.

*Author for correspondence

pertaining to the equatorial and meridional directions were recorded over the 2θ ranges of $3\text{--}72^\circ$ and $8\text{--}52^\circ$, respectively, at scanning intervals of 0.02° , using a curved position sensitive detector. As the plane of the diffractometer circle was horizontal, the fibres were mounted vertically to record the equatorial reflections and then rotated by 90° to the horizontal position to record the meridional reflections. To estimate the $2\theta_{\max}$ and the half-width, ω , of the reflections, Lorentzian² functions were fitted on the observed profiles by the least squares method.

The unit cell parameters a and b were estimated from the two most intense reflections, (200) and (110), respectively. In the diffraction patterns the meridional reflection (006) was found to be slightly asymmetric. As a result, the error in fitting a Lorentzian² function was comparatively high. Hence, in order to avoid high values of standard deviation, the calculation of the c -value was based only on the (004) reflection. In order to elicit information on the azimuthal spread of the equatorial reflections, transmission Laue photographs were recorded both prior to and after exposure for 6 h to ultrasonic waves.

Tensile testing of single filaments was carried out on a Zwick universal testing machine using a cross head speed of 2.5 mm/min and chart speed of 60 mm/min. Only fibres which had 6 h of exposure to ultrasonic waves were compared with the as-received fibres. For both the sets 50 filaments were examined and the average value of strength and modulus were determined.

3. Results and discussion

3.1 Crystallographic data

Figures 1(a) and (b) present the equatorial and the meridional diffraction patterns recorded prior to axial compression. In figures 2(a) and (b), the patterns from fibres exposed to ultrasonic waves for 1, 3 and 6 h, respectively have been compared. As was reported earlier (Iyer and Vijayan 1996), increase in the duration of exposure to ultrasonic waves represents a corresponding increase in the extent of compression. Thus the patterns in figure 2 are from fibres compressed to different extents, the 6 h set being the most compressed. The overall similarity between the patterns from the as-received and the compressed fibres shows that the basic crystal structure of the fibre is unaffected by the process of compression. Careful examination of the patterns, however, indicates that compression leaves a residual effect, viz. shifts in the 2θ values of both equatorial and meridional reflections. Table 1 presents the observed shifts (Δ) in the 2θ values along with the respective e.s.d.'s (cr). It is found that with the exception of the basal plane reflections from fibres agitated for 1 h, for

all the other reflections, the ratio Δ/σ is ≥ 3.0 . Though subtle, the observed shifts in the 2θ values are therefore statistically significant.

Figure 3 presents the percentage variation in the unit cell dimensions with the extent of compression. The most conspicuous feature is the anisotropic deformation of the unit cell. Whereas the c -axial length manifests a contraction, the basal plane dimensions register an expansion. Both the effects increase progressively with increase in the extent of compression.

As is well known, Kevlar crystallizes in a monoclinic unit cell, with the chain axis parallel to the unique axis which in this case is the crystallographic c -axis (Northolt 1974). Molecules of PPTA or poly(*p*-phenylene terephthalamide) of which Kevlar fibres are made of (Meredith 1975), assume a fully extended all-trans conformation along the c -direction. Therefore, the c -axial length of the unit cell corresponds to the end-to-end dimension of a PPTA monomer in the crystal structure. Any change in the c -axial length should hence imply corresponding changes in the structural characteristics

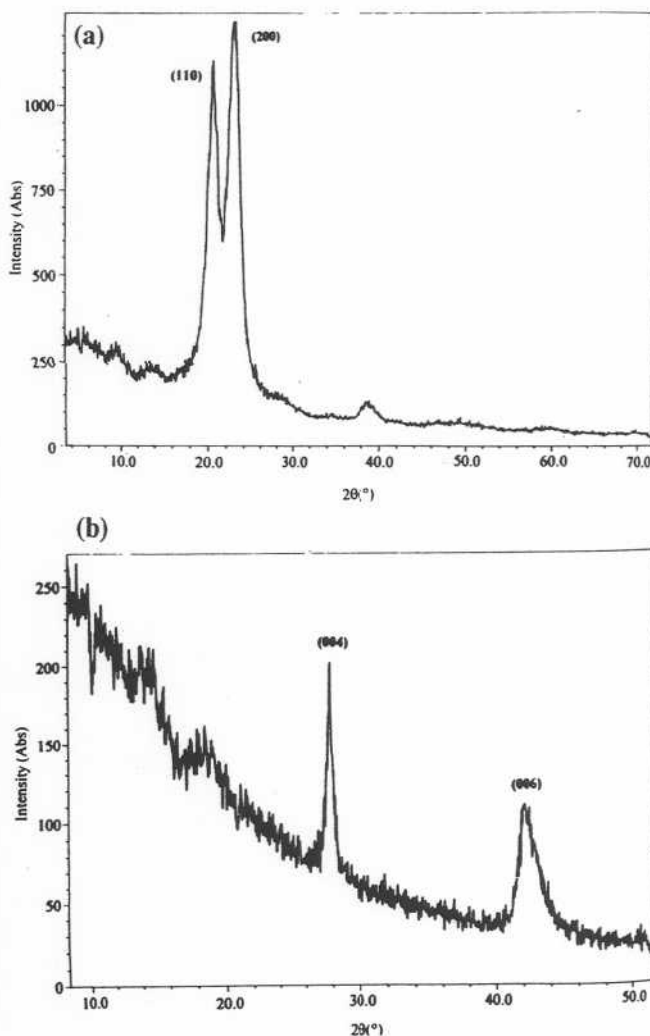


Figure 1. X-ray diffraction patterns prior to ultrasonic compression: (a) equatorial and (b) meridional.

along the chain direction. Figure 3 shows that for the most compressed sample used in this study, the c -axis length reduces by $\approx 0.4\%$. The observed reduction may be associated with the occurrence of the following types of deformations:

- (I) Slight changes in the initial torsional angles, bond lengths and angles introduced during the process of compression, tantamounting to a 0.4% contraction.
- (II) Randomly introduced conformational changes from the initial all-trans conformation.
- (III) Chain bending similar to that reported for a poly(p -phenylene) oligomer. Based on molecular dynamics simulations, Socci *et al* (1993) correlate the negative axial thermal expansion coefficient of rigid-rod like chains of a sexiphenyl to a wavelike deformation along the chain. Introduction of similar deformations in PPTA, which is also rigid-rod like, during compression cannot be ruled out. Figure 4 is a schematic representation of the proposed wave like deformation.

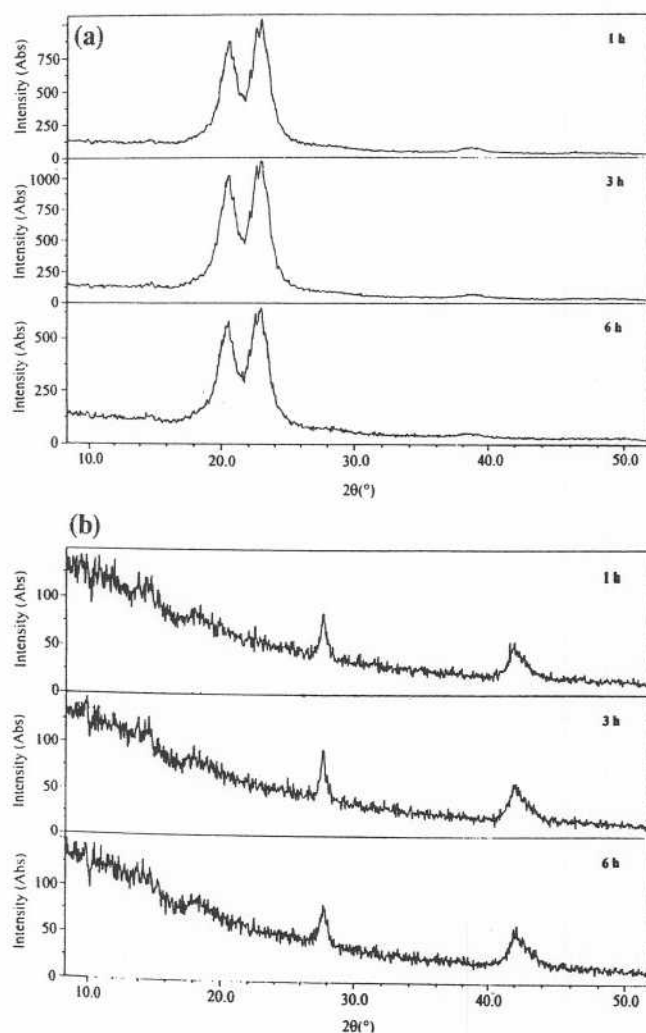


Figure 2. X-ray diffraction patterns from fibres compressed to various extents. The duration of compression has been marked: (a) equatorial and (b) meridional.

Admittedly, the above mentioned types of correlation are only predictive in nature. Occurrence of any of the above-mentioned deformations can be confirmed only by carrying out further analysis.

The observed reduction in the c -length of compressed fibres is in striking contrast with the theoretical predictions of Lacks (1996) according to whom, a larger dimension should be observed along the chain axis. It must be pointed out that a direct comparison of the present experimental data with Lacks' theoretical results is not valid for the following reasons: Lacks' calculations

Table 1. The observed shifts in the 2θ ($^\circ$) values along with the e.s.d.'s.

t_{cum} (h)	$\Delta(2\theta_{110})$	$\sigma(\Delta)$	$\Delta/\sigma(\Delta)$
As-received	—	—	—
1	0.0131	0.0078	1.70
3	0.0871	0.0098	8.90
6	0.1165	0.0103	11.3
	$\Delta(2\theta_{200})$	$\sigma(\Delta)$	$\Delta/\sigma(\Delta)$
As-received	—	—	—
1	0.0085	0.0062	1.37
3	0.1099	0.0077	14.3
6	0.1368	0.0085	16.1
	$\Delta(2\theta_{004})$	$\sigma(\Delta)$	$\Delta/\sigma(\Delta)$
As-received	—	—	—
1	0.0412	0.0120	3.40
3	0.0608	0.0120	5.05
6	0.1027	0.0178	5.80

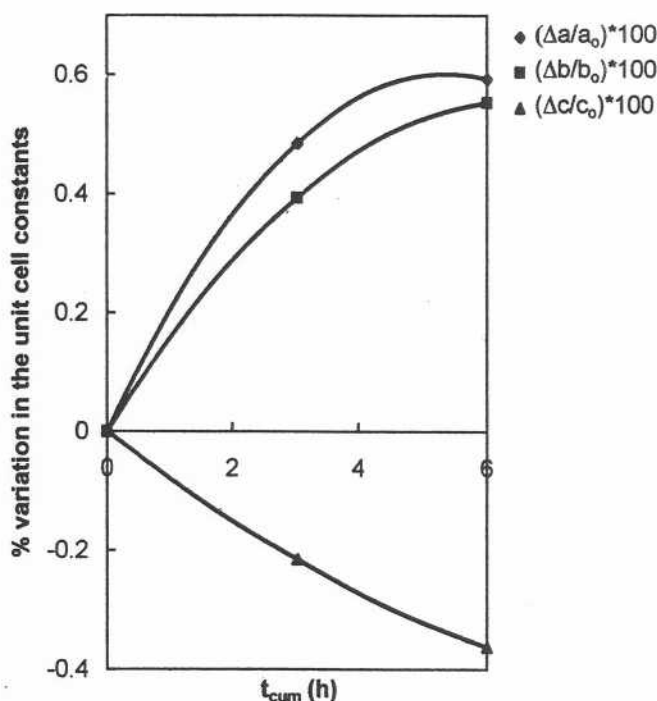


Figure 3. Variation of the unit cell constants in ultrasonically compressed fibres.

concern an infinite crystal of PPTA whereas the present study is on fibres of finite length. The physical characteristics of a fictitious, infinitely long crystal are understandably different from those of a fibre. The former represents an ideal condition whereas the latter is a synthesized product with inherent defects. Presence of defects can affect the behaviour of the fibre. Kevlar, as is well known, has a paracrystalline structure (Northolt and Aartsen 1977), a skin-core differentiation (Morgan et al 1983) and surface impurities (Vijayan 1987). Features like these which differentiate the fibre from an infinitely long crystal can account for the observed difference between Lacks' predictions and the present experimental data. Secondly, Lacks considers a crystal failed in compression, whereas the present X-ray data are from compressed but not compressively failed samples.

As mentioned earlier, the effect of compression on the basal plane dimensions (figure 3) is strikingly different from that on the chain axis. Both *c*- and *b*-axial lengths increase with compression. In the crystal structure of PPTA, the *a*-direction corresponds to a concentration of van der Waals' interaction between adjacent layers. Our earlier studies have shown that *a*-dimension increases readily with thermal ageing (Iyer and Vijayan 1994). The present data (figure 3(b)) shows that similar sensitivity is characteristic of compression also. Such a recurrence establishes the vulnerability of the weak inter-layer interactions in the crystal structure of PPTA to deforming agencies which could be either thermal or ultrasonic in nature.

The observed increase in the *b*-value is in support of the deformation model shown in figure 4. It may be

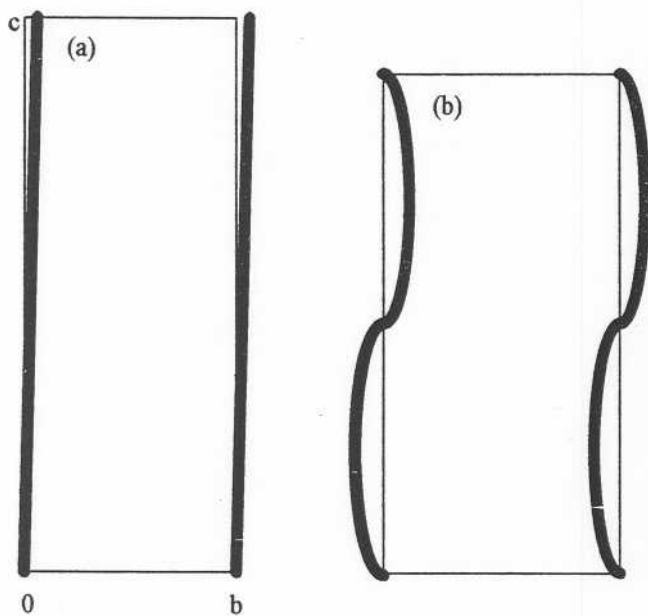


Figure 4. Schematic representation of the wave-like deformation of chains. Orientation prior to (a) and after (b) compression.

appreciated that it requires more space to pack the deformed chains along the crystallographic *b*-direction than the undeformed ones. In the crystal structure of Kevlar, adjacent chains along the *b*-direction interact to form a network of hydrogen bonds all of which are nearly parallel to the crystallographic *b*-direction. The possibility that the increase in the *b*-length represents a corresponding weakening of the hydrogen bonds cannot indeed be ruled out. However, since the polyamides have an inherent propensity to form interchain hydrogen bonds, it is difficult to comprehend such a weakening of the already existing network of hydrogen bonds. It must also be mentioned that in contrast with the compressed fibres, in the case of the thermally aged fibres (Iyer and Vijayan 1994), the *b*-dimension of the unit cell did not register any significant change. If heating did not weaken the hydrogen bonds, it may not be inappropriate to assume that compression did not also weaken the hydrogen bonds; in which case, the observed increment in the *b*-value could be attributed entirely to the axial deformation of molecules.

Figure 5 compares the percentage increase in the area of the basal plane with the corresponding volume of the unit cell. Despite the reduction in the *c*-length, the unit cell of compressed fibres registers an overall increase in volume. Such an enlargement is due, primarily, to the anisotropic nature of axial deformations. Interestingly, the anisotropic dimensional changes of the unit cell of compressed fibres bear a resemblance to the macro dimensional changes observed during heating of Kevlar fibres. Rojstaczer *et al* (1985) have reported a negative axial CTE of $-5.7 \times 10^{-6}/^{\circ}\text{C}$ and a positive transverse CTE of 66.3×10^{-6} for the temperature range 20–80°C. Comparison of the strains along the fibre axis, however, shows that the resemblance is only qualitative. In the former case, the strain is -0.363% whereas in the latter case for $T=30^{\circ}\text{C}$ it is only -0.017% .

The parameter which is determined by the 2θ values is the angular separation $\Delta(2\theta) = (2\theta)_{(200)} - (2\theta)_{(110)}$. Figure 6 depicts the observed reduction in the $\Delta(2\theta)$ value with

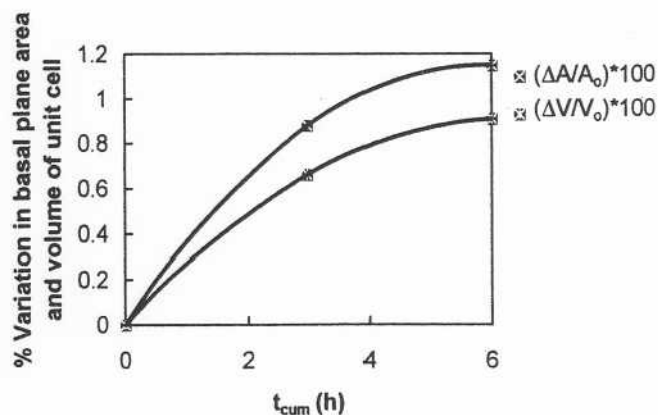


Figure 5. Compression induced changes in the basal plane area and unit cell volume.

axial compression. Such a closing up of the equatorial reflections suggests reduction in the tensile strength of the fibre (Shubha *et al* 1991). Details of the experimentally measured tensile strength will be presented in the subsequent section.

In addition to the 20 values, the half width and the azimuthal spread of reflections also manifest compression induced changes. Figure 7 depicts the progressive sharpening of the equatorial reflections, a behaviour very similar to that observed in thermally aged fibres (Iyer and Vijayan 1994). Ultrasonic agitation thus appears to have a beneficial, annealing type of effect on the basal plane of the crystal structure. In striking contrast with the equatorial reflections, the meridional reflections exhibit progressive broadening (figure 8) which may be associated with the introduction of microstrain and/or fragmentation of crystallites along the chain direction. Introduction of microstrain is indeed in keeping with

the concept of deformation along the chain direction mentioned earlier.

Figure 9 presents the increase in the azimuthal spread of reflections recorded from fibres compressed by 6 h of ultrasonic exposure. Such an increase is indicative of misalignment of polymer chains about the fibre axis which in turn suggests deterioration in the tensile modulus of the fibre.

The above mentioned X-ray observations provide an unambiguous evidence that the effect of macro compression penetrates upto the crystal lattice. X-ray data further suggest deterioration in tensile properties which indeed has been confirmed experimentally, the details of which follow.

3.2 Tensile characteristics

Experimentally measured tensile strength and modulus of ultrasonically compressed fibres (table 2) conform well with the X-ray observations. As in the case of thermally aged fibres (Parimala and Vijayan 1993), the reduction in tensile strength is more than the modulus, the reductions being - 17% and 10.4%, respectively. Similar reduction in tensile strength has been reported by Deteresa *et al* (1984) and Dobb *et al* (1981), both of whom have studied Kevlar fibres compressed by different methods. Deteresa *et al* (1984) have shown that application of 100 cycles to 1.2% compressive strain causes 10% loss in tensile strength. Dobb *et al* (1984) report 24% loss in tensile strength of fibres subjected to 1000 flexural cycles.

Figure 10 compares typical load-extension curves recorded from the as-received and ultrasonically compressed fibres. It is observed that the curve from ultrasonically compressed fibres is similar in shape to that recorded prior to compression. Deteresa *et al* (1984), on the other hand, report a 'dramatic change' in the shape, in the initial portion of the stress-strain curve during

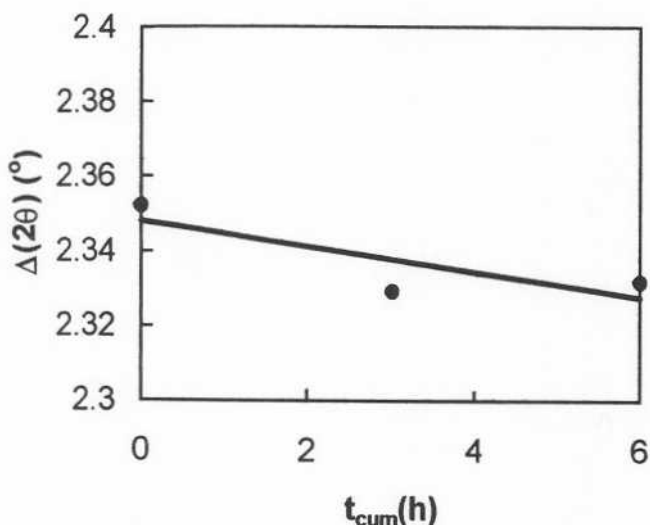


Figure 6. Compression induced reduction in the angular separation of the equatorial reflections.

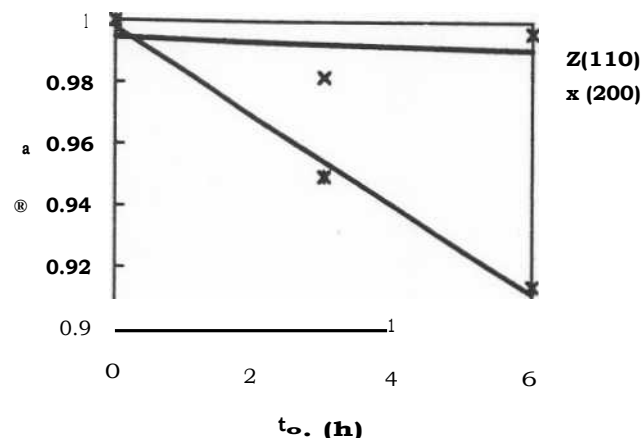


Figure 7. Reduction in the half-width values of the equatorial reflections.

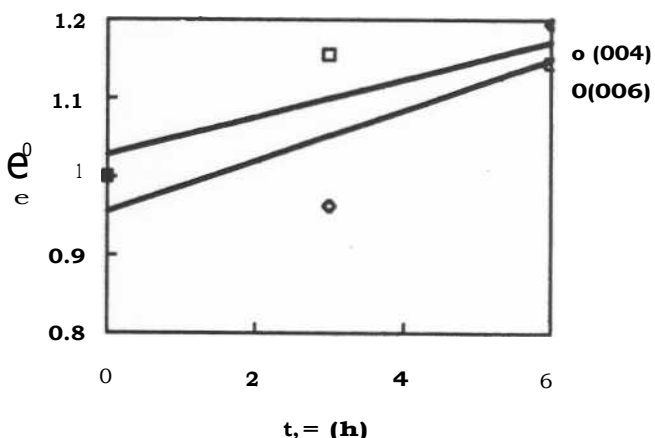


Figure 8. Increase in the half-width values of the meridional reflections.

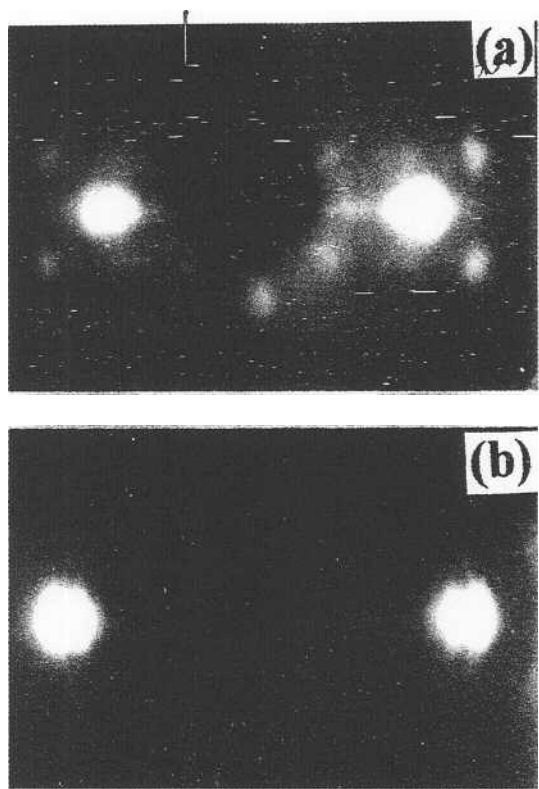


Figure 9. Comparison of the azimuthal spreads before (a) and after (b) compression.

Table 2. Comparison of tensile strength and modulus of fibres prior to and after compression.

Sample	Tensile strength (GPa)	Tensile modulus (G Pa)
As-received	3.25(16)	106(6)
Compressed	2.70(33)	95(5)

the first tensile loading following compression. Absence of such differences between the curves in figure 10 may be associated with the differences in the experimental conditions used for tensile testing. Deteresa et al (1984) have utilized a slow pulling rate of 1 mm/min and a gauge length of 50 mm. In contrast, in the present study, the cross head movement was comparatively fast, viz. 15 mm/min and the gauge length was also less viz. 25 mm. It is likely that consequent to these differences, the fine features of the load-extension curve seen by Deteresa et al (1984) were missed out in the present study.

4. Conclusion

The effect of macro axial compression of Kevlar 49 fibres percolates upto the crystal lattice. The unit cell suffers an anisotropic deformation. Whereas the c-axis

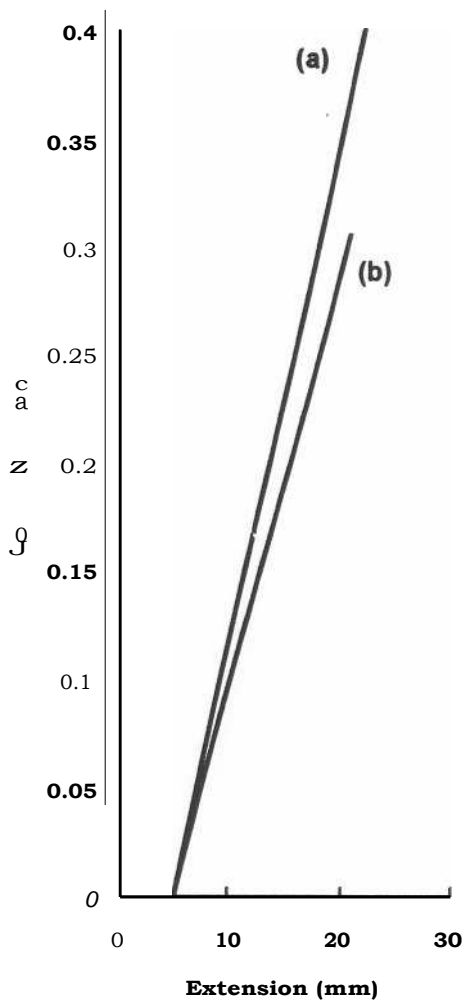


Figure 10. Comparison of the load-extension curves of fibres prior to (a) and after (b) compression.

length (chain axis) contracts, the transverse ab-plane enlarges. X-ray data suggest possible deformations along the chain direction. The reductions in the tensile modulus and strength of compressed fibres are in qualitative agreement with the compression induced structural changes.

Acknowledgements

RVI and KV thank the Aeronautical Research and Development Board of India for sanctioning a project under which the work presented in this paper was carried out. RVI and KS thank the CSIR for the award of senior research fellowships. KS and TIN thank the DST for funding. The authors wish to sincerely thank Drs Sudha Mahadevan and A Giridhar for providing the facilities to carry out the ultrasonic exposure. The authors

indeed are grateful to Dr A K Singh for encouragement and support.

References

- Detcresa S J, Allen S R, Farris R J and Porter R 5 1984 .1. *Mater. Sci.* 19 57
- Dobh M G, Johnson D J and Saville B P 1977 *J. Pohym. Sci. Pot yin, Phys. Ed. 15* 2201
- Dobb M G, Johnson D J and Saville B P 1981 *Polymer* 22 960
- Greenwood J II and Rose P G 1974 *J Mater. Sci.* 9 1809
- Iver R V and Vijayan K 1994 in *Polymer science recent advances* I (ed.) I S Bhardwaj (New Delhi: Allied) p. 362
- Iyer R V and Vijayan K 1996 *Curr Sci.* 71 398
- Lacks D J 1996 *J. Mater. Sci.* 31 5885
- McGarry F J and Moalfi J E 1991 *Polymer* 32 1816
- Meredith R 1975 *Text, IProgr.* 7 No. 4
- Morgan R J, Pruneda C 0 and Steele W J 1983 *J. Pohmr. Sri. Palem. Pln'S. Ed. 21* 1757
- Northolt M G 1974 *Eur. Pot vin. J* 10 799
- Northolt M G and van Aartsen J J 1977 *J Polyr. Sri. Polym. Symp.* 58 238
- Parimala H V and Vijayan K 1993 *J. Mater. Sci. Lett* 12 99
- Rojstaczer S, Cohn D and Maron G 1985 *J. Mater. Sci. Len.* 4 1233
- Shubha M, Pariniala li V and Vijayan K 1991 *J. Mater, Sci. Len.* 10 1377
- Socci E P, Farmer B 1L and Adams W W 1993 *J. Polvm. Sci. Polvm. Phys. Ed. 31* 1975
- Vijayan K 1987 *Curr. Sci.* 56 1055